

Improvement of Mechanical Properties and Corrosion Resistance of Friction Stir Welded Joints Made of Dissimilar Aluminum Alloys Through Scandium-Enriched Alloy Powder Incorporation

Samadhanam Karanam Raju^{1*}, Nallu Ramanaiah¹

¹ Department of Mechanical Engineering, Andhra University College of Engineering, Visakhapatnam – 530003, India

* Corresponding author's e-mail: samadhanamraju@andhrauniversity.ac.in

ABSTRACT

Friction stir welding (FSW) is a widely utilized process for joining aluminum alloys due to its ability to produce high-quality welds with excellent mechanical properties. In this study, the effect of adding Scandium enriched (Al-1Sc-0.3Zr) alloy powder on the FSW of AA2024 and AA6351 alloys was investigated. The experimentation was carried out at different speeds of 800, 1200, and 1600 rpm while maintaining a welding speed of 35 mm/min and an axial load of 3 kN. The master alloy powder was added to the base materials prior to welding, and the resulting welds were characterized using optical microscopy, scanning electron microscopy, hardness testing, tensile testing, and corrosion testing. At 800 rpm, the tensile strength increased from 200.7 MPa without powder to 241.8 MPa with powder and hardness values were notably higher in samples with powder, such as increasing from 98.3 HV without powder to 115.33 HV with powder at 1200 rpm. The addition of the Scandium enriched powder significantly improved the tensile strength, hardness, and corrosion resistance of the welds compared to welds produced without the use of this powder. The findings of this study suggest that incorporating Scandium enriched powder into the FSW process can effectively enhance the mechanical and corrosion properties of AA2024 and AA6351 alloy welds, thereby improving the overall performance of the welding process.

Keywords: FSW performance, scandium enriched powder, welding speed, axial load, mechanical properties, weld characterization.

INTRODUCTION

Friction Stir Welding is a solid-state welding technique invented in 1991 by Wayne Thomas (Thomas et al., 1991) at The Welding Institute in the United Kingdom used to join two or more metals without using any filler material or melting the metals. Unlike traditional welding methods, FSW (Figure 1) does not involve the melting of the metals being joined. Instead, a rotating cylindrical tool with a pin and a shoulder is inserted into the work pieces that are clamped together (Prabhu et al., 2018). The tool is rotated at high speeds and moved along the joint line, generating heat and pressure that softens the metal to a plastic state, allowing the tool to stir the metals together and

create a homogeneous joint. The tool's shoulder helps to distribute the heat generated during the process, preventing excessive localized heating and minimizing distortion. The pin, which is positioned at the centre of the shoulder, penetrates the work pieces and stirs the softened material, creating a mechanically sound joint without any voids or defects. The advantages of FSW include high welding speed, low distortion, reduced heat input, and improved mechanical properties of the joint (Mishra, 2018). Because the metals are not melted, there is no need for any filler material, reducing the cost and time required for the welding process. The low heat input also reduces the risk of distortion and prevents the formation of brittle intermetallic compounds, resulting in improved

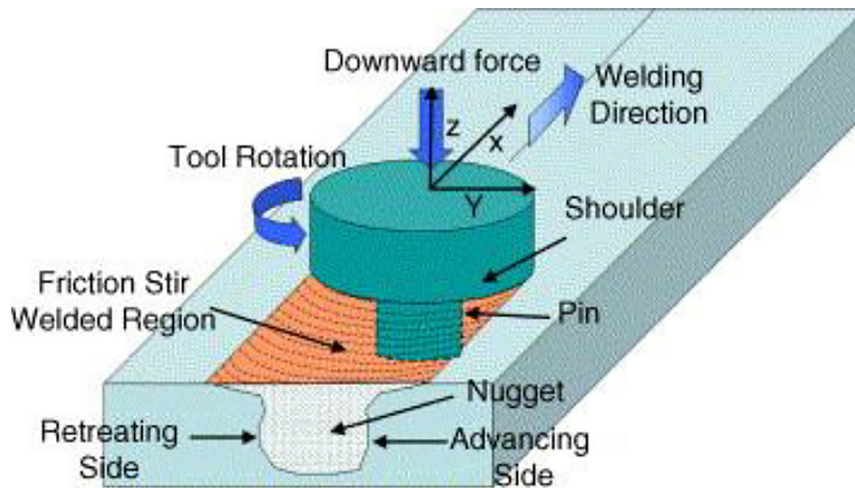


Figure 1. FSW schematic diagram [Prabhu et al., 2018]

mechanical properties of the joint. FSW can be used to join a wide range of materials, including aluminum alloys, magnesium alloys, copper alloys, titanium alloys, and even some plastics. In this study, aluminum alloys AA2024 and AA6351 are selected as the base materials for welding. However, aluminum alloys, particularly those containing copper and magnesium, can pose challenges during welding due to the formation of brittle intermetallic compounds and potential susceptibility to corrosion. By incorporating scandium-enriched powder into the FSW process, this research aims to mitigate some of these challenges and enhance the mechanical and corrosion properties of the welded joints. The addition of scandium offers the potential to refine the microstructure, improve material flow, and increase the overall performance of the welded joints, addressing some of the inherent issues associated with welding aluminum alloys. It has proven to be a reliable and efficient method for joining aluminum alloys, including aerospace, automotive, marine, and structural applications (Kluz et al., 2019).

Several studies have investigated the microstructural, mechanical, and corrosion properties of aluminum alloys welded with the addition of scandium. Arunkumar, D., and KS Vijay Sekar. (2024) explored the influence of scandium interlayer on the mechanical and metallurgical properties of friction stir welded joints between dissimilar AA1200-H14 and AA6061-T6 alloys. Results show that optimal settings yield maximum tensile strength and improved frictional heat observations. SEM analysis reveals fine and equiaxed grains, indicating enhanced mechanical properties and microstructural refinement

with the inclusion of scandium interlayer. Senthamaraikannan et al. (2023) investigated the use of FSW with a scandium (Sc) interlayer to join AA5052-H32 and AA6061-T6 alloys, commonly used in military-grade applications like ship hull constructions and armoured helicopters. FSW parameters including tool rotation speed, welding speed, and tool pin depth are optimized to improve material flow and reduce brittleness. A 2 mm Sc interlayer is added to enhance weld joint strength. Shine and Subbaiah (2020) found that the inclusion of scandium led to microstructure refinement and improved mechanical properties such as hardness and tensile strength. Jiang et al. (2014) observed that scandium and zirconium additions significantly influenced the alloy's microstructure and mechanical properties, resulting in increased hardness and strength. Kumar et al. (2022) examined the influence of FSW parameters on dissimilar joints and found that corrosion resistance decreased with increased traverse speed but improved with higher rotational speed. Sudhakar and Srinivas (2019) investigated the corrosion behavior of FSW butt welds and observed accelerated corrosion in the weld joint compared to the base alloys, with the presence of precipitates contributing to corrosion pit formation. D'Urso et al. (2017) noted that process parameters significantly affected tensile strength, hardness, and corrosion resistance, with higher rotational speed and lower traverse speed leading to improved properties. Additionally, Fahimpour et al. (2012) found that FSW joints exhibited superior corrosion resistance compared to gas tungsten arc welding joints, attributed to the unique

microstructure induced by FSW. These studies collectively underscore the importance of scandium addition and FSW parameters in enhancing the microstructural, mechanical, and corrosion properties of aluminum alloys. In this work, scandium-enriched powder is incorporated into the stir zone of the samples, followed by FSW, resulting in improved performance.

MATERIALS

The materials used in the study are dissimilar aluminum alloys, specifically AA6351-T6 and AA2024-T6 plates. These alloys were selected due to their distinct compositions and mechanical properties, offering a platform for investigating the effects of Scandium-enriched alloy powder incorporation on friction stir welded joints. Each plate measured 100 × 75 × 6.3 mm in dimensions. A rotating tool applied a consistent normal load during the welding process. Parameters included three rotational speeds (800 rpm, 1200 rpm, and 1600 rpm) while maintaining a constant welding speed of 35 mm/min and a vertical normal load of 3 kN. These parameters were selected based on a combination of literature review, preliminary trials, and the specific requirements of the materials used (AA2024 and AA6351). These parameters are known to effectively balance the heat generation and material flow necessary for producing

sound welds in aluminum alloys. The tool, made from H13 tool steel, featured an 18 mm diameter shoulder, a 6 mm diameter pin, and a tip height of 6 mm. These parameters and geometries were selected to ensure consistency and accuracy in the FSW process simulation, facilitating the evaluation of material behavior and weld quality. The chemical compositions were determined using spectroscopy, and the mechanical properties of the base materials were measured. The description of the materials utilized in the study comprises four key tables: Table 1 presents the chemical composition of AA6351-T6, detailing the elemental composition crucial for understanding its properties and behavior. Similarly, Table 2 provides the chemical composition of AA2024-T6, offering insight into its elemental makeup. Table 3 outlines the mechanical properties of the base metals, providing essential data on their tensile strength, yield strength, and other mechanical characteristics. Lastly, Table 4 presents the chemical composition of H13 steel, the material used in constructing the tool for the friction stir welding process.

METHODOLOGY

The methodology for this study involves several key steps to investigate the effects of incorporating scandium-enriched powder into the

Table 1. Chemical composition of the material AA6351-T6; material chemical composition by weight%

| Component | Si | Fe | Cu | Mn | Mg | Al |
|-----------|---------|-----|-----|---------|---------|------|
| % | 0.6–1.3 | 0.6 | 0.1 | 0.4–1.0 | 0.4–1.2 | Bal. |

Table 2. Chemical composition of the material AA2024-T6

| Component | Si | Fe | Cu | Mn | Mg | Zn | Al |
|-----------|-------|------|-----|------|------|------|------|
| % | 0.046 | 0.17 | 4.7 | 0.65 | 1.56 | 0.11 | Bal. |

Table 3. Base metal mechanical properties

| Base metal | UTS (MPa) | YS (MPa) | Elongation (%) | Vicker's hardness (VHN) (0.1kgf) |
|-------------|-----------|----------|----------------|----------------------------------|
| AA6351-T6 | 329 | 272 | 11.7 | 100.46 |
| AA2024-T351 | 421 | 307 | 19.6 | 119 |

Table 4. Chemical composition of H13 steel

| Component | C | Mn | Si | P | S | Cr | Mo | Ni | V | Fe |
|-----------|-------|-------|--------|-------|-------|-------|--------|-------|-------|------|
| % | 0.331 | 0.321 | 1.0183 | 0.014 | 0.011 | 5.127 | 1.0176 | 0.049 | 0.989 | Bal. |

FSW process of aluminum alloys AA2024 and AA6351. Firstly, the base materials, AA2024 and AA6351, are prepared in the form of rectangular plates sized $100 \times 75 \times 6.3$ mm. The scandium-enriched powder is then added to the surface of the plates prior to welding. The FSW process is conducted using a FSW machine with specific parameters: rotational speeds of 800, 1200, and 1600 rpm, a constant welding speed of 35 mm/min, and an axial load of 3 kN. During welding, a rotating cylindrical tool with a pin and shoulder is inserted into the workpieces, generating heat and pressure to soften the metals and create a homogeneous joint. The resulting welds are characterized using various techniques, including optical microscopy, scanning electron microscopy, hardness testing, and tensile testing, to evaluate the microstructural, mechanical, and corrosion properties of the welded joints.

EXPERIMENTATION

Al-1Sc-0.3Zr master alloy ingot

Al-1Sc-0.3Zr master alloy is a specialized material that plays a crucial role in improving the properties of aluminum alloys. This master alloy is composed of aluminum (Al) as the base metal, with added scandium (Sc) and zirconium (Zr) elements. The unique combination of these elements imparts remarkable enhancements to the mechanical, microstructural, and corrosion properties of aluminum alloys, making it an essential component in various industries, including aerospace, automotive, and marine engineering. The powder used in this study was prepared through a filing process. In this method, bulk Al-1Sc-0.3Zr alloy material (Figure 2) was carefully filed down into fine particles, resulting in the production of the powder (Figure 3a). The filing process ensured the creation of uniform

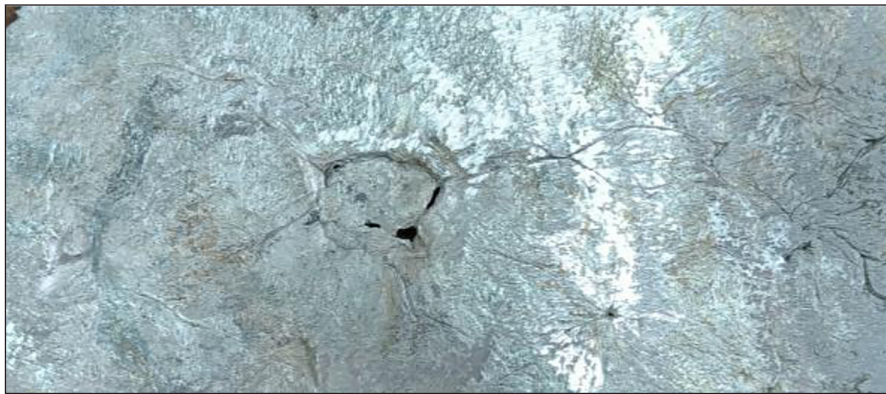
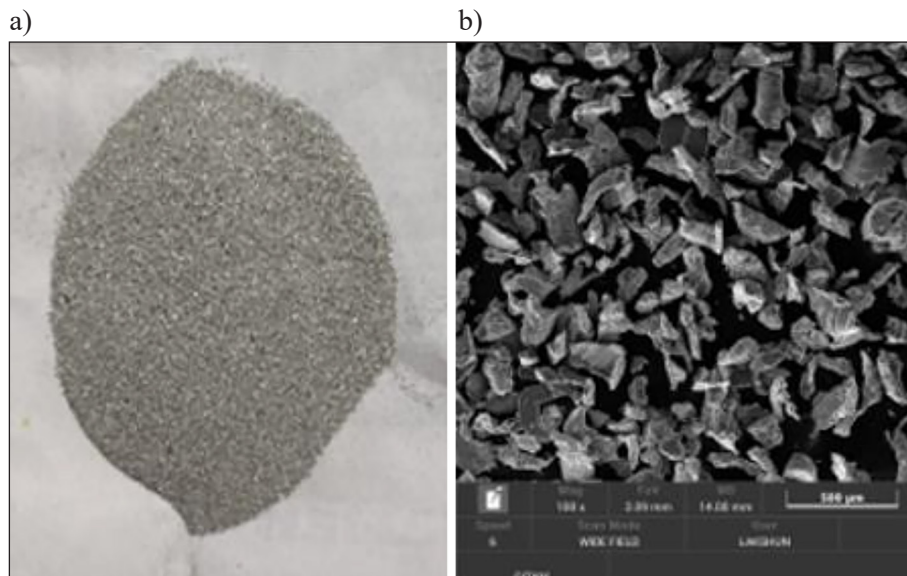


Figure 2. Al-1Sc-0.3Zr Ingot



Figures 3. (a) Scandium enriched powder, (b) SEM analysis of the powder

and small-sized particles, which were essential for effective dispersion and incorporation into the weld material during the friction stir welding process. This method was chosen for its simplicity and ability to produce a high-quality powder suitable for the experimental procedures. The manual powder addition technique was chosen for its simplicity, allowing for precise control over the amount of powder added and its placement within the stir zone. The hands-on approach facilitated a practical and effective method of incorporating the Al-1Sc-0.3Zr powder, enabling a detailed evaluation of its impact on the resulting weld properties. The Scandium enriched powder was subjected to scanning electron microscopy (SEM) analysis (Figure 3b) to investigate its morphology and microstructure. The SEM analysis revealed a fine and uniform distribution of Scandium particles within the powder matrix. The surface of the powder exhibited a homogeneous distribution of particles with irregular shapes and sizes, indicating good dispersion and mixing of the Scandium alloy within the powder matrix. Table 5 provides the composition of the Al-1Sc-0.3Zr master alloy.

Figures 4 and 5 show the dissimilar aluminum alloys AA6351-T6 and AA2024-T6 before welding, where Figure 4 depicts the plates with holes and Figure 5 illustrates these holes filled with

scandium-enriched alloy powder. Figure 6, on the other hand, displays the samples without any holes, prepared for the friction stir welding process.

FSW setup

The FSW setup employed for joining dissimilar aluminum alloys AA2024 and AA6351 involves a robust and precisely controlled apparatus. The FSW machine is equipped with specialized tooling designed to accommodate the dissimilar nature of the alloys. Clamping mechanisms ensure secure fixation of the AA2024 and AA6351 plates of size 100 × 75 × 6.3 mm, facilitating consistent material flow during welding. The tool, featuring a threaded shoulder and a tapered pin with a wear-resistant material, is configured to provide the necessary rotational and axial forces. Real-time monitoring and feedback systems ensure accurate control of welding parameters, including rotation speed, welding speed, and axial force. This setup ensures the generation of defect-minimized, high-quality joints between dissimilar aluminum alloys, enabling comprehensive investigations into joint properties and microstructural characteristics. Figure 7a shows the welding machine, a critical component in

Table 5. Composition of Al-1Sc-0.3Zr

| Element | Sc | Zr | Fe | Si | Al |
|-------------|------|------|------|------|---------|
| Composition | 1.08 | 0.32 | 0.19 | 0.01 | Balance |



Figure 4. Samples with holes along stir zone for powder addition

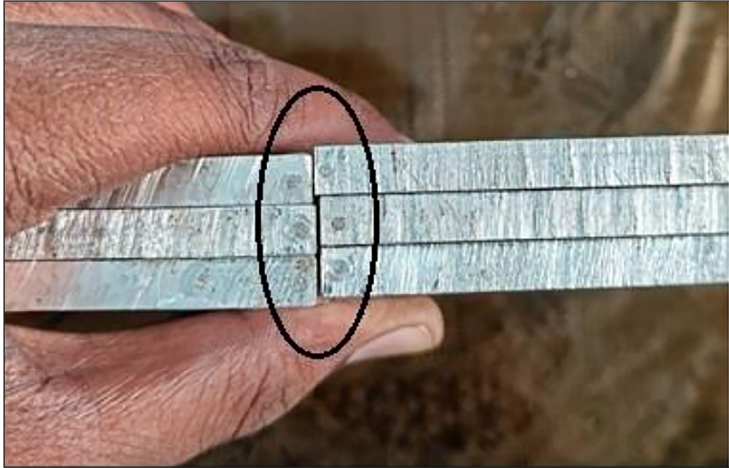
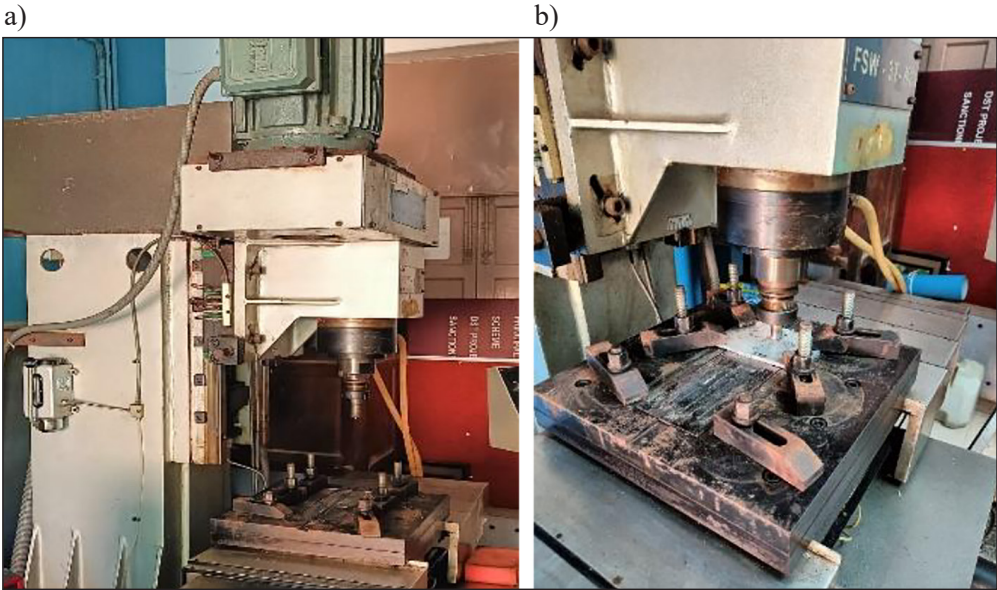


Figure 5. Powder added in the holes



Figure 6. Samples without holes



Figures 7. FSW setup: (a) machine, (b) plates fixed

the FSW process, equipped to apply the necessary rotational speed, welding speed, and normal load for the experiment. Figure 7b depicts the aluminum alloy plates, AA6351-T6 and AA2024-T6, securely fixed in position on the machine bed, ready for the welding process. Figure 8 illustrates the FSW tool made of H13 tool steel, featuring a pin with a diameter of 6mm and a depth of 6mm. Figure 9 shows the fabricated FSW welds at three different speeds 800, 1200 and 1600 rpm at 35 mm/min welding speed and 3 kN axial force without (above three figures) and with Scandium enriched alloy powder

(below three figures) and Table 6 shows the different weld appearances. Table 6 illustrates the visual appearances of friction stir welded (FSWed) samples at different rotational speeds, both with and without powder. It showcases the weld appearances at 800, 1200, and 1600 rpm without powder, as well as at 800 and 1200 rpm with powder.

RESULTS

Tensile testing

Figures 11a and 11b display the tensile specimens of friction stir welded samples prepared for mechanical testing. Figure 11a shows the tensile specimens of an FSWed sample without the addition of scandium-enriched alloy powder. Figure 11b presents the tensile specimens of an FSWed sample with the incorporation of scandium-enriched alloy powder which underwent cutting using CNC Milling in accordance with the ASTM E8 standards (shown below Figure 10) before and after testing respectively. The tensile test is performed on tensile testing machine (INSTRON Make-Figure 12).

Tensile test results

The investigation focused on the effects of tool rotational speed (800, 1200, and 1600 rpm) on the tensile strength, yield strength, and elongation of

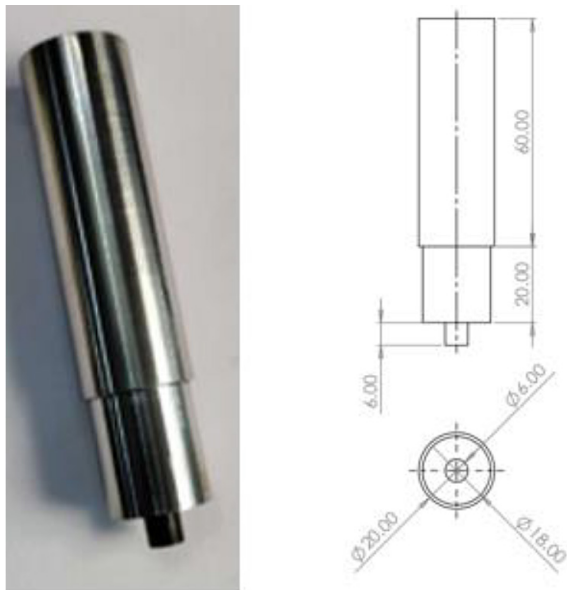


Figure 8. Cylindrical FSW tool

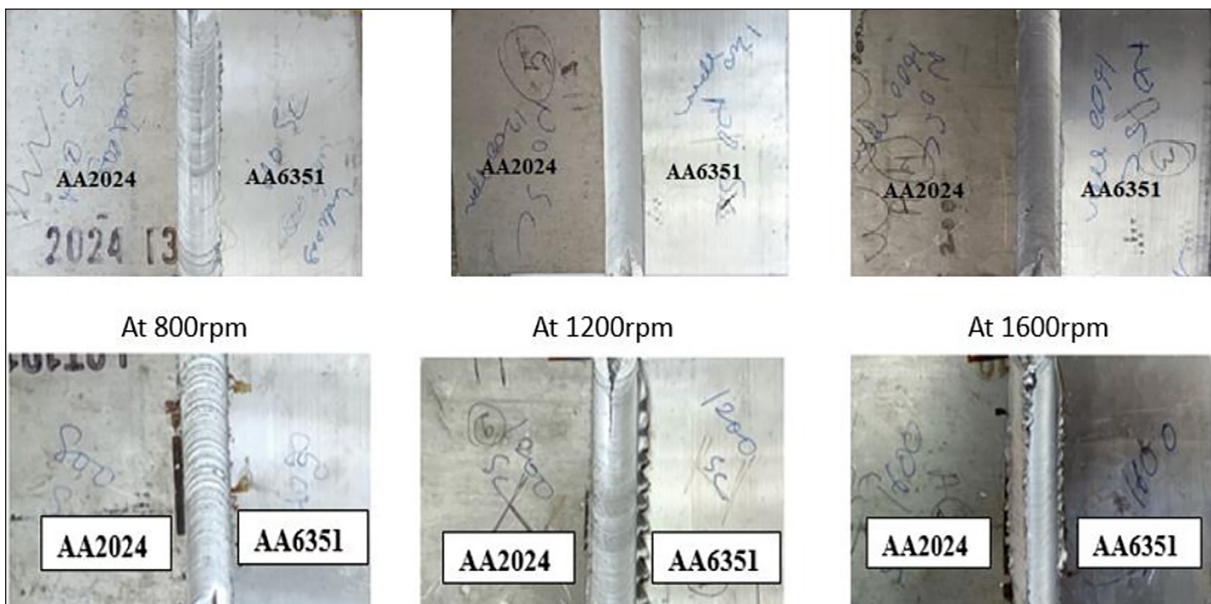




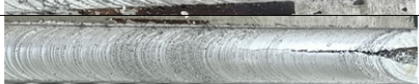



Figure 9. Fabricated joints

Table 6. Weld appearances

| Description | Weld appearance |
|----------------------------|--|
| At 800 rpm without powder |  |
| At 1200 rpm without powder |  |
| At 1600 rpm without powder |  |
| At 800 rpm with powder |  |
| At 1200 rpm with powder |  |
| At 1600 rpm with powder |  |

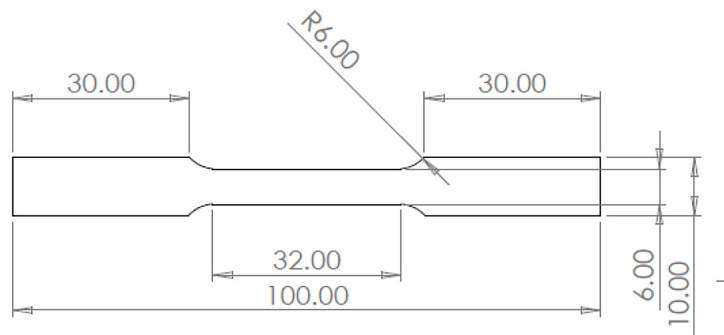
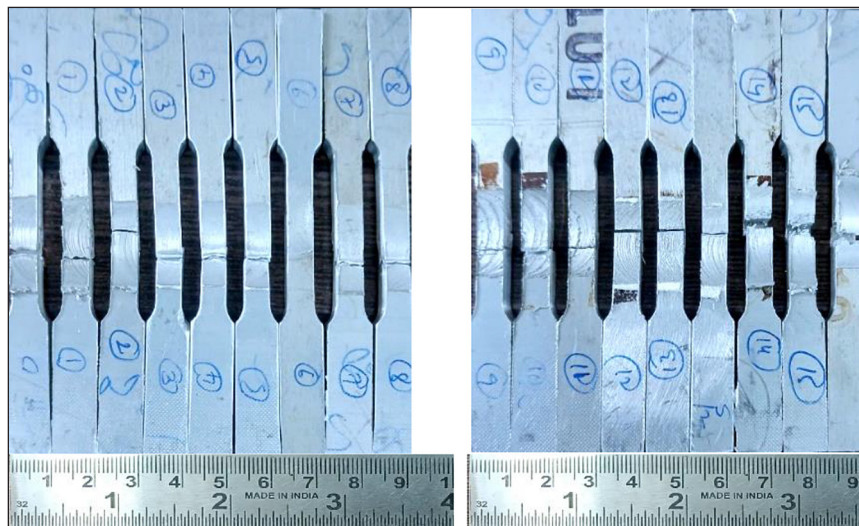


Figure 10. Tensile specimen drawing



Figures 11. Tensile specimens of FSWed samples: (a) without powder, (b) with powder

welded samples, conducted at a constant speed of 35 mm/min and an axial force of 3000 N (Table 7). Three samples were made for each test at the same

parameters. The addition of scandium-enriched powder to the FSW process significantly improved the mechanical properties of the aluminum



Figure 12. Tensile test set up

Table 7. Tensile test results with and without Scandium enriched powder

| Rotational speed (rpm) | Without scandium enriched powder | | | With scandium enriched powder | | |
|------------------------|----------------------------------|----------|--------------|-------------------------------|----------|--------------|
| | UTS (MPa) | YS (MPa) | % Elongation | UTS (MPa) | YS (MPa) | % Elongation |
| 800 | 200.7 | 167.25 | 5.3 | 241.8 | 201.5 | 4.56 |
| 1200 | 244.5 | 202.84 | 6.5 | 275.5 | 229.58 | 5.65 |
| 1600 | 232.5 | 193.75 | 4.8 | 256.5 | 213.75 | 4.27 |

alloy joints across all tested rotational speeds. At a rotational speed of 800 rpm, the ultimate tensile strength (UTS) increased from 200.7 MPa to 241.8 MPa, while the yield strength (YS) improved from 167.25 MPa to 201.5 MPa. Similarly, at 1200 rpm, the UTS increased from 244.5 MPa to 275.5 MPa and the YS from 202.84 MPa to 229.58 MPa. At 1600 rpm, the UTS rose from 232.5 MPa to 256.5 MPa, and the YS from 193.75 MPa to 213.75

MPa. However, this improvement in strength was accompanied by a reduction in ductility. The percentage elongation decreased from 5.3% to 4.56% at 800 rpm, from 6.5% to 5.65% at 1200 rpm, and from 4.8% to 4.27% at 1600 rpm. The observed increase in both tensile and yield strengths with scandium addition is attributed to microstructure refinement, resulting in grain size reduction and enhanced dispersion of strengthening precipitates.

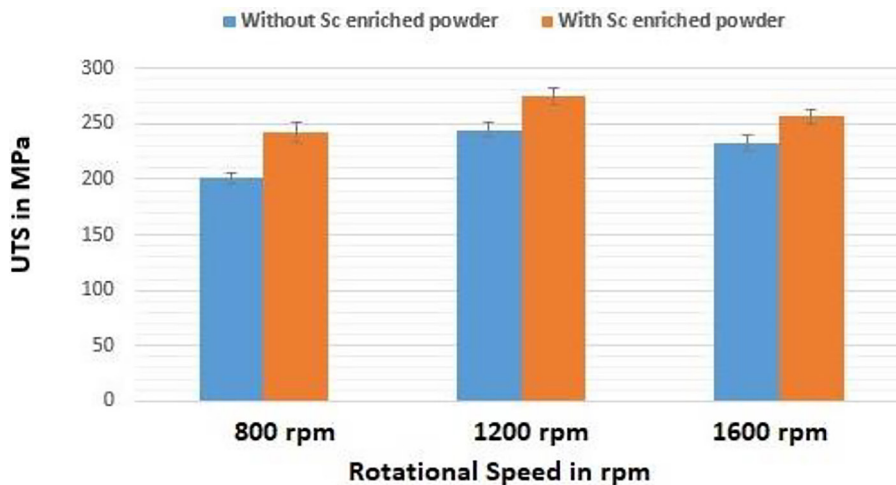


Figure 13. Tensile strength comparison

While scandium contributes to increased strength, it might also influence ductility, leading to slightly reduced elongation percentages. These findings are consistent with the trends reported in the literature, such as those by Zhu et al. (2023) and Rao and Ramanaiah (2018), who observed similar enhancements in mechanical properties with scandium and zirconium micro-alloying in aluminum alloys. These comparisons highlight that scandium significantly enhances the mechanical properties of aluminum alloys, reinforcing the results of the current study. Figure 13 shows the tensile strength comparison.

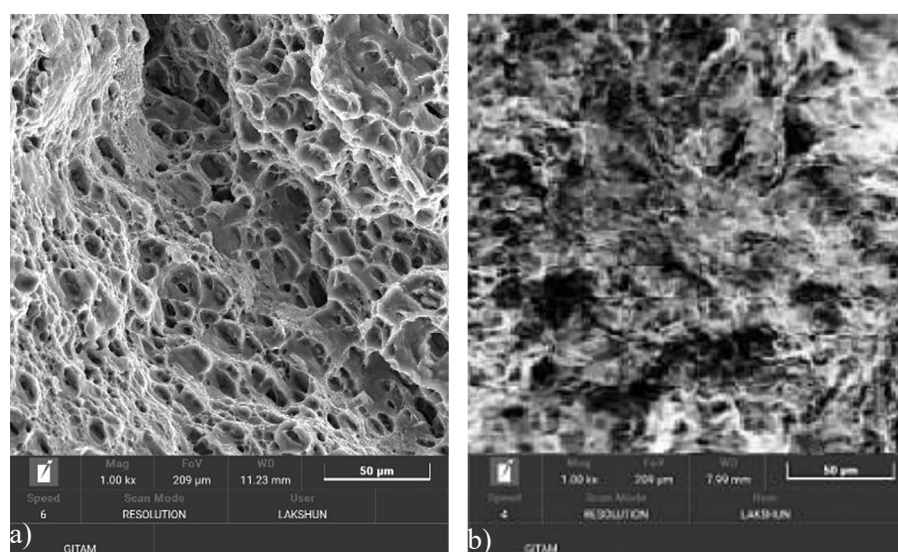
Fracture analysis

Fracture analysis was performed on FSWed samples produced at a rotational speed of 1200 rpm, comparing those with and without Scandium enriched powder. Samples without powder (Figure 14a) exhibited a higher number of dimples on the fracture surface, indicating a ductile fracture mode due to significant plastic deformation before failure. This aligns with the lower tensile strength and hardness values recorded for these samples, suggesting reduced overall material strength. In contrast, samples with Scandium enriched powder (Figure 14b) showed no dimples on the fracture surface. This demonstrates that the addition of scandium-enriched powder significantly reduces the ductility of the welded samples. Despite this, these samples exhibited higher tensile strength and hardness values, indicating

improved mechanical properties facilitated by the reinforcement effect of the powder.

Hardness

The Vickers hardness test was conducted using a load of 1 kilogram-force applied for a duration of 10 seconds in accordance with ASTM E384 standard. The Vickers hardness numbers (HV) were measured at the stir zone of FSW samples, both with and without Scandium-enriched powder, at rotational speeds of 800 rpm, 1200 rpm, and 1600 rpm. For samples without powder, the hardness values exhibited variation with rotational speed, ranging from 55.93 HV at 800 rpm to 98.3 HV at 1200 rpm, and then slightly decreasing to 91.9 HV at 1600 rpm. Conversely, incorporating powder into the FSW process resulted in consistently higher hardness values across all speeds, ranging from 67.2 HV at 800 rpm to 115.33 HV at 1200 rpm, and then decreasing slightly to 105.5 HV at 1600 rpm. These findings suggest that the addition of Scandium-enriched powder enhances the hardness of the FSWed samples, indicating potential improvements in mechanical properties such as strength and wear resistance. The observed trend of increasing hardness with the addition of powder highlights the effectiveness of Scandium in refining the microstructure and promoting the formation of stronger intermetallic phases within the weld matrix. This enhancement in hardness underscores the potential for utilizing Scandium-enriched powder to enhance the mechanical performance of friction



Figures 14. Fracture analysis of FSWed samples: (a) without powder, (b) with powder

stir welded joints, particularly in aluminum alloys like AA6351 and AA2024. The observed variation in hardness values with changes in the tool’s rotational speed underscores the significant influence of process parameters on the mechanical properties of friction stir welded joints. In this study, an increase in rotational speed led to a corresponding increase in hardness values for samples without powder, peaking at 1200 rpm before slightly decreasing at 1600 rpm. Conversely, incorporating Scandium-enriched powder consistently yielded higher hardness values across all rotational speeds. The relationship between rotational speed and hardness can be attributed to several factors. Firstly, at lower rotational speeds, there is insufficient heat generation and material flow, resulting in incomplete grain refinement and intermetallic phase formation, leading to lower hardness values. As the rotational speed increases, more heat is generated, promoting greater material flow and enhanced mixing of alloying elements, which contribute to finer grain size and more uniform distribution of strengthening precipitates, consequently increasing hardness. However, beyond a certain threshold, excessive rotational speeds can lead to excessive heat generation and material softening, potentially resulting in a decrease in hardness. Additionally, the incorporation of Scandium-enriched powder enhances the formation of fine and uniformly

distributed precipitates, further increasing hardness values across all rotational speeds. This is consistent with the results of Senthamaraiannan et al. (2023), who reported increased hardness from 60 HV to 70 HV when scandium was incorporated into AA5052-H32 and AA6061-T6 alloy welds. These findings are consistent with observations made by Shine and Subbaiah (2020) in their study on AA5083 aluminum alloy, where the addition of scandium increased yield stress and hardness values while reducing the percentage elongation of the welded joint. The below Table 8 shows the hardness results.

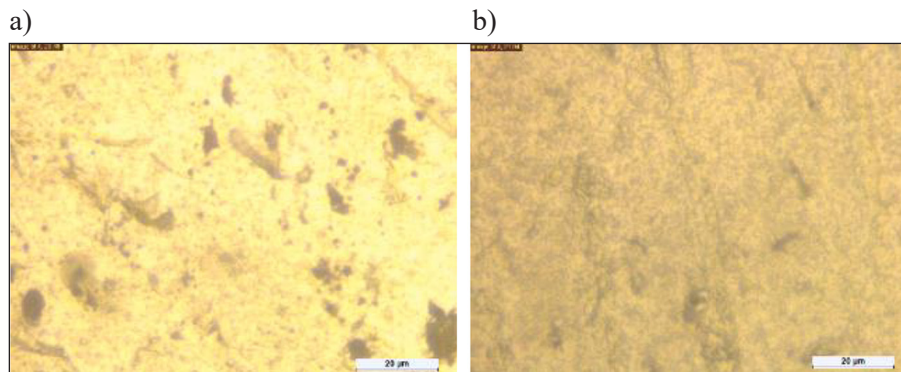
Microstructures

The examination of microstructures provides valuable insights into the distribution of precipitates within the material. In the context of aluminum alloys, specifically AA 2024 (Figure 15a) and AA 6351 (Figure 15b), the precipitates identified are Al_2Cu and Mg_2Si , respectively. Notably, the microstructural analysis indicates a uniform and even dispersion of these precipitates throughout the entire material matrix.

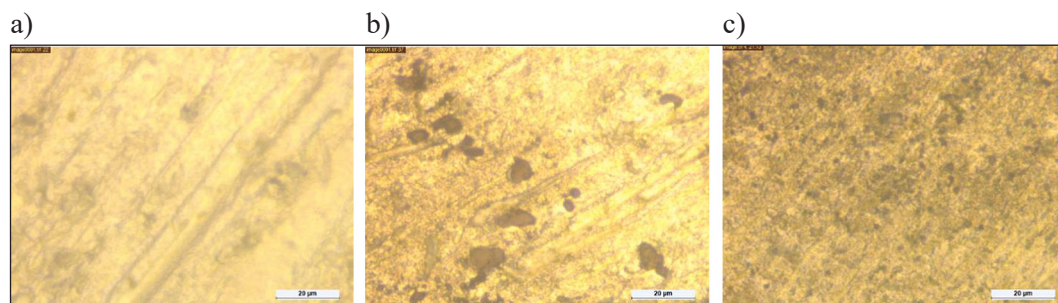
OM, SEM, and corrosion tests were conducted exclusively for the FSWed samples without powder at 800, 1200, and 1600 rpm, as well as for those with powder at 800 and 1200 rpm. The FSWed sample with powder at 1600 rpm

Table 8. Hardness test results

| Sample | Vicker’s hardness number (980 mN for 10s) |
|---|---|
| FSWed sample without powder at 800 rpm | 55.93 |
| FSWed sample without powder at 1200 rpm | 98.3 |
| FSWed sample without powder at 1600 rpm | 91.9 |
| FSWed sample with powder at 800 rpm | 67.2 |
| FSWed sample with powder at 1200 rpm | 115.33 |
| FSWed sample with powder at 1600 rpm | 105.5 |



Figures 15. Microstructures of welded parts made of aluminum alloy: (a) AA2024, (b) AA6351



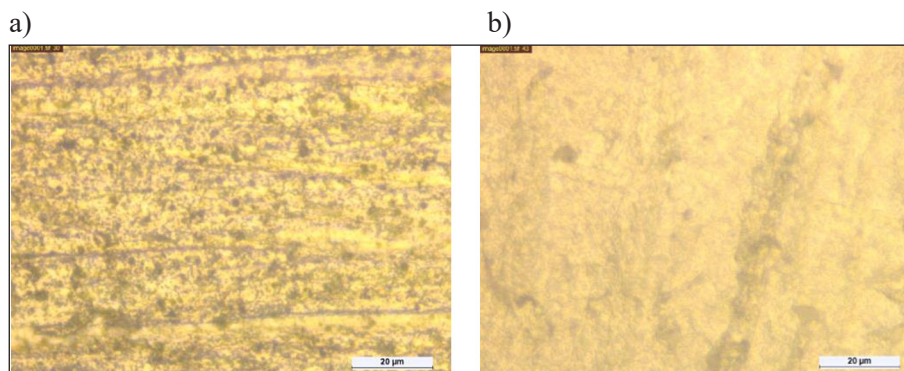
Figures 16. Microstructures of FSWed samples without powder at: (a) 800 rpm, (b) 1200 rpm, (c) 1600 rpm

was excluded from these tests due to its poor quality. This sample exhibited significant defects and inconsistencies during the fabrication process, which compromised its structural integrity and made it unsuitable for reliable testing. At 800 rpm, the OM examination reveals distinct features characterized by grain coarsening and irregular grain boundaries (Figure 16a). The larger grain sizes observed indicate a less refined microstructure, potentially attributable to lower rotational speeds resulting in inadequate mixing and plastic deformation during the welding process. Increasing the rotational speed to 1200 rpm presents a notable shift in microstructural characteristics (Figure 16b). The OM study indicates a refinement in grain structure compared to the 800 rpm samples. However, irregular grain boundaries persist, suggesting a suboptimal level of dispersion strengthening mechanisms. Further elevation of the rotational speed to 1600 rpm showcases continued improvement in microstructural refinement (Figure 16c). The OM analysis demonstrates finer grain sizes and a more uniform distribution, indicative of enhanced dispersion strengthening mechanisms. However, certain irregularities may still be present, albeit to a lesser extent compared to lower rotational speeds. At 800 rpm with alloy powder, the OM study

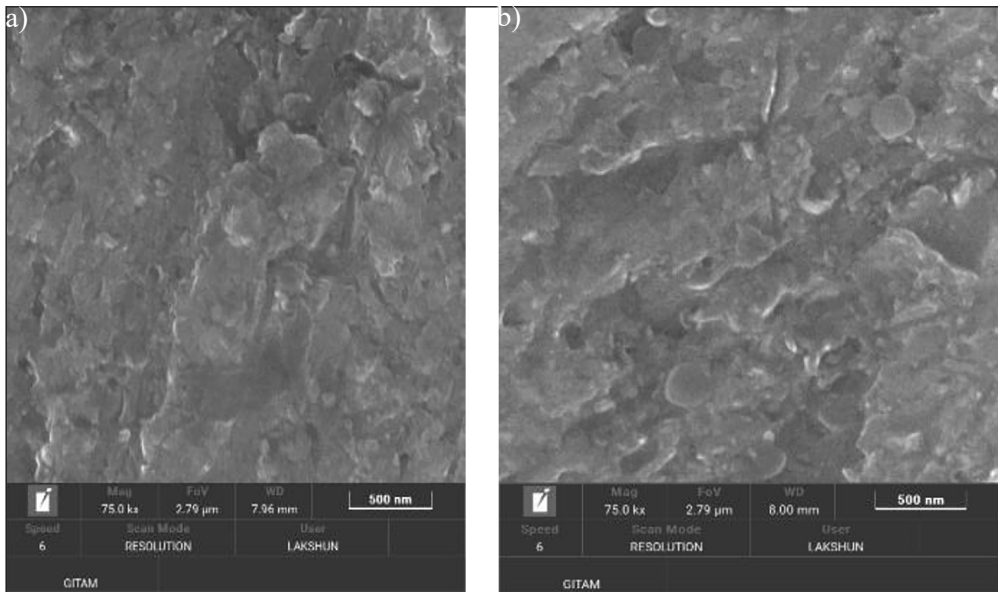
reveals a refined microstructure with finer grain sizes and more uniform distribution compared to samples without powder at the same rotational speed (Figure 17a). The presence of alloy powder contributes to the formation of precipitates within the weld matrix, enhancing grain refinement and strengthening mechanisms. Similarly, at 1200 rpm with alloy powder, the OM analysis showcases further refinement and modification of the microstructure (Figure 17b). Finer grain sizes and more uniform distribution of precipitates, facilitated by the Scandium-enriched alloy powder, contribute to enhanced mechanical properties and overall weld integrity. The dynamic recrystallization that occurred in the weld nugget zone due to the tool pin profile action resulted in smaller grain sizes in this region. The addition of a scandium enriched powder further contributed to the reduction in grain growth.

SEM

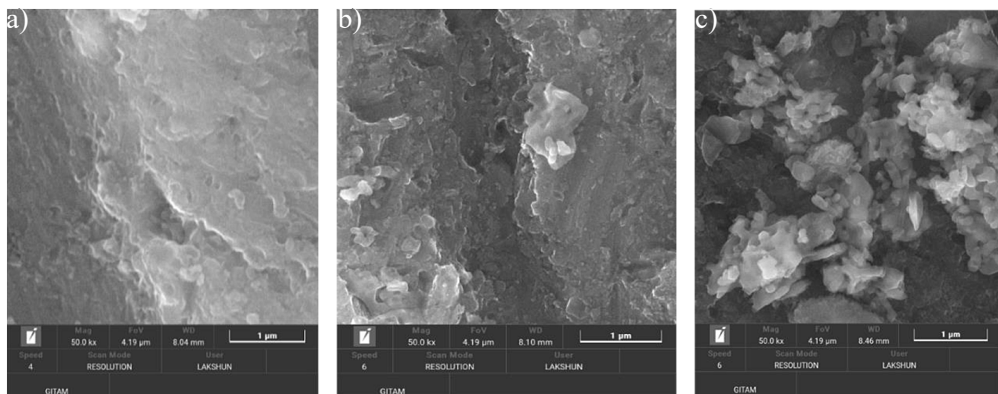
The SEM analysis of AA6351 and AA2024 base materials (Figures 18a and 18b) revealed characteristic microstructures typical of each alloy. AA6351 exhibited a uniform microstructure with distinct grain boundaries and dispersed precipitates, while AA2024 displayed a more



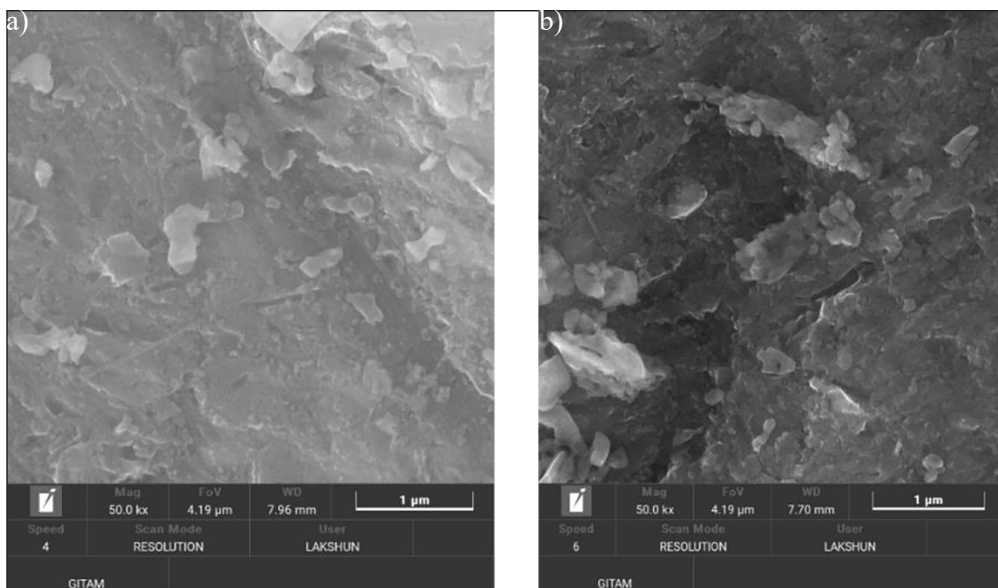
Figures 17. Microstructures of FSWed samples with powder at: (a) 800 rpm, (b) 1200 rpm



Figures 18. SEM analysis of base materials: (a) AA6351, (b) AA2024



Figures 19. SEM analysis of FSWed samples without powder at: (a) 800 rpm, (b) 1200 rpm



Figures 20. SEM analysis of FSWed samples with powder at: (a) 800 rpm, (b) 1200 rpm

heterogeneous microstructure with intermetallic particles dispersed throughout the matrix. At 800 rpm, SEM images revealed a microstructure characterized by relatively larger grain sizes and irregular grain boundaries (Figure 19a). The absence of powder led to limited dispersion strengthening mechanisms, resulting in a less refined microstructure with diminished mechanical properties. Increasing the tool rotational speed to 1200 rpm yielded notable changes in the microstructural features (Figure 19b). Here, SEM analysis unveiled further grain coarsening and irregularities in grain boundaries, indicative of a less refined microstructure compared to lower rotational speeds. This observation suggests that while the rotational speed influences the weld microstructure, without the addition of alloy powder, the refinement of the microstructure remains limited. At 1600 rpm, SEM examination exhibited similar trends with continued grain coarsening and irregular grain boundaries (Figure 19c). Despite the higher rotational speed, the absence of alloy powder failed to mitigate these microstructural deficiencies, resulting in a less refined weld matrix. In contrast, FSWed samples with the inclusion of Scandium-enriched alloy powder were investigated at rotational speeds of 800 and 1200 rpm. At 800 rpm, SEM images depicted a refined

microstructure characterized by finer grain sizes and more uniform grain boundaries compared to samples without powder (Figure 20a). The presence of alloy powder facilitated the formation of finer precipitates within the weld matrix, contributing to improved mechanical properties and overall weld integrity. Similarly, at 1200 rpm, SEM analysis revealed further refinement of the microstructure with the addition of alloy powder (Figure 20b). Finer grain sizes and more uniform distribution of precipitates, including Al₃Sc and Al₃Zr, were observed throughout the weld matrix. These findings underscore the significant role of Scandium-enriched alloy powder in enhancing the microstructural characteristics and mechanical properties of FSWed samples.

CORROSION TESTING

Figures 21 and 22 show that the Tafel plots of the base materials and the FSWed samples with and without powder. The corrosion test experiments were conducted in sea water solution using ASTM G61 standard procedures. The corrosion rates of the samples reveal significant differences in their corrosion resistance. Table 9 presents a detailed comparison of corrosion rates among different samples, highlighting significant

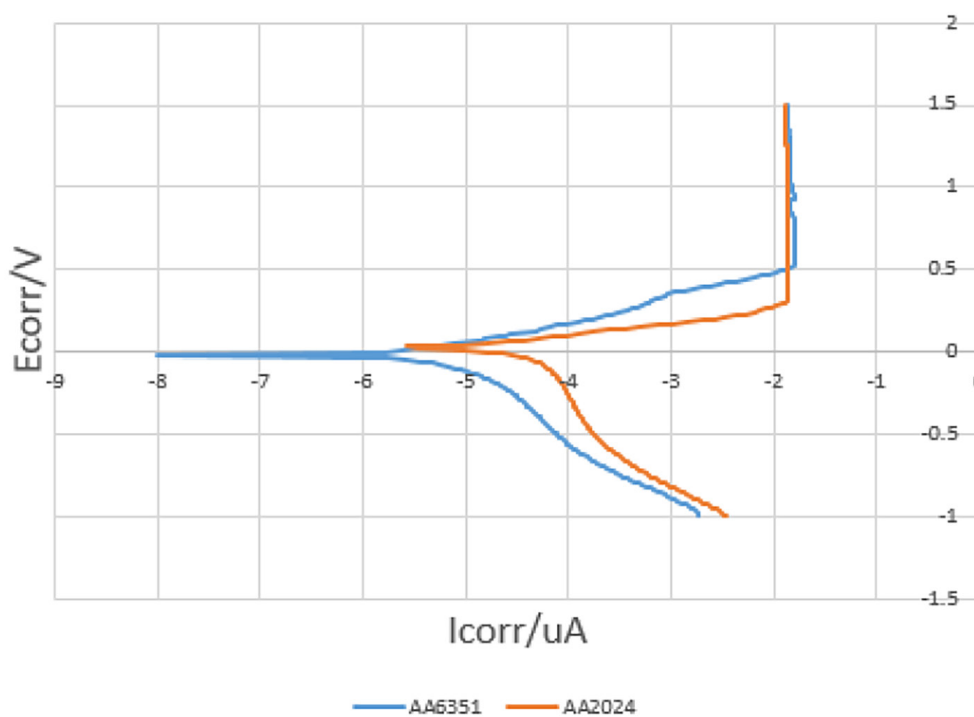


Figure 21. Corrosion testing of base materials

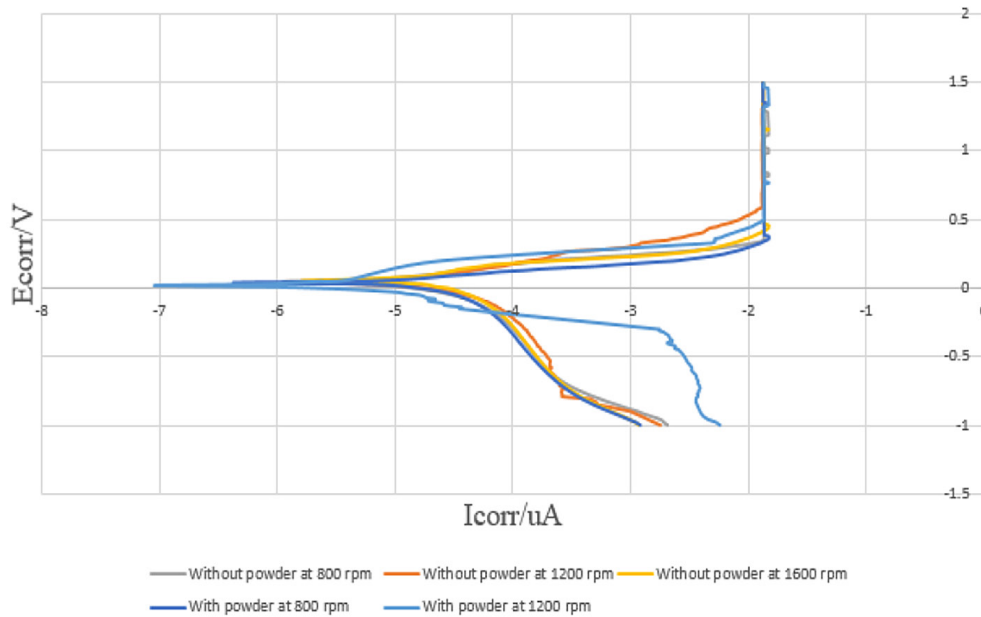


Figure 22. Corrosion testing of FSWed samples with and without powder

Table 9. Corrosion test results

| Sample | Corrosion rate (mm/year) |
|---|--------------------------|
| AA6351 (Base material) | 0.0068 |
| AA2024 (Base material) | 4.31 |
| FSWed sample without powder at 800 rpm | 4.94 |
| FSWed sample without powder at 1200 rpm | 1.27 |
| FSWed sample without powder at 1600 rpm | 4.92498 |
| FSWed sample with powder at 800 rpm | 4.92996 |
| FSWed sample with powder at 1200 rpm | 0.0079 |

variations in their corrosion resistance. AA6351 emerges as the most corrosion-resistant base material with a rate of 0.0068 mm/year, contrasting sharply with AA2024, which exhibits a significantly higher corrosion rate of 4.31 mm/year. In the case of friction stir welded (FSWed) samples without powder, corrosion rates vary notably with rotation speed. At 800 rpm, the corrosion rate measures 4.94 mm/year, whereas at 1200 rpm, it decreases to 1.27 mm/year. Interestingly, the sample at 1600 rpm shows a corrosion rate similar to that at 800 rpm, at 4.92498 mm/year. FSWed samples with powder present contrasting outcomes: at 800 rpm, the corrosion rate matches the non-powdered sample at the same speed, at 4.92996 mm/year. However, at 1200 rpm, the corrosion rate notably drops to 0.0079 mm/year, signifying a significant enhancement in corrosion resistance under these conditions. These results underscore the effectiveness of

scandium-enriched powder in mitigating corrosion susceptibility in FSWed aluminum alloys. Ahmad et al. (2001) demonstrated similar findings in their study on scandium alloyed Al 5052, where the corrosion behavior was significantly improved in a neutral sodium chloride solution.

CONCLUSIONS

The addition of scandium-enriched powder in friction stir welded aluminum alloys demonstrates significant enhancements across multiple performance metrics.

- Improvement in tensile strength: at 800 rpm, the addition of Scandium enriched powder resulted in a noticeable enhancement in tensile strength, increasing from 200.7 MPa without powder to 241.8 MPa with powder. Similarly, at 1200 rpm, the tensile strength

exhibited a significant improvement, rising from 244.5 MPa without powder to 275.5 MPa with powder. Furthermore, at 1600 rpm, the tensile strength increased from 232.5 MPa without powder to 256.5 MPa with powder.

- Enhancement in hardness: at 800 rpm, the inclusion of Scandium enriched powder led to a notable increase in hardness, rising from 55.93 HV without powder to 67.2 HV with powder. Similarly, at 1200 rpm, the hardness values exhibited a significant improvement, increasing from 98.3 HV without powder to 115.33 HV with powder. Furthermore, at 1600 rpm, the hardness increased from 91.9 HV without powder to 105.5 HV with powder.
- Microstructural refinement: optical microscopy (OM) and scanning electron microscopy (SEM) analyses showed refined grain structures and uniform distribution of Scandium particles in the weld matrix, indicating enhanced weld quality and integrity.
- Corrosion resistance: at 1200 rpm, the corrosion rate significantly decreased in FSWed samples with Scandium enriched powder, highlighting improved corrosion resistance under specific processing conditions. For example, the corrosion rate in the welds with powder was significantly lower than in those without powder.

These findings collectively demonstrate that the addition of Scandium enriched powder to the FSW process of AA2024 and AA6351 alloys leads to substantial improvements in tensile strength, hardness, and corrosion resistance, with the optimal results observed at a rotational speed of 1200 rpm.

Acknowledgements

The authors express their sincere gratitude to the Department of Mechanical Engineering, Andhra University, for their invaluable support and provision of essential resources, which were instrumental in the successful execution of this research. Furthermore, heartfelt thanks are extended to JNTU Kakinada for granting permission to conduct Friction Stir Welding (FSW) experimentation using their FSW machine and also GITAM, Visakhapatnam for granting permission to conduct the characterization, thereby facilitating the practical validation of our study.

REFERENCES

1. Thomas, W.M., Nicholas, E.D., Needam, J.C., Murch, M.G., Templesmith, P. and Dawes, C.J. GB Patent Application No. 9125978.8, December 1991 and US Patent October 1995; 5460317.
2. Prabhu, Subramanya R., Shettigar, A., Herbert, M., and Raoet, S. Multi response optimization of friction stir welding process variables using TOPSIS approach. IOP Conference Series: Materials Science and Engineering. IOP Publishing, 2018; 376(1).
3. Mishra, A. Friction Stir Welding of Dissimilar Metal: A Review. 2018. Available at SSRN: <https://ssrn.com/abstract=3104223>
4. Arunkumar, D., and Sekar K.S.V. Influence of scandium interlayer on the mechanical and metallurgical characteristics of friction stir welded AA1200-H14/Sc/AA6061-T6. Materials Research Express 11.1 2024; 016507.
5. Balamurugan, S., and Krishnamoorthy, J. Material flow and mechanical properties of friction stir welded AA 5052-H32 and AA6061-T6 alloys with Sc interlayer. Materials Testing 65.7 2023; 1127–1142.
6. Shine, K., and K. Subbaiah. Experimental Investigation of the Addition of Scandium on the Microstructural and Mechanical Properties of Friction Stir Welded AA5083 Aluminium Alloy. Tierärztliche Praxis 2020; 40.
7. Kosturek, R., Śnieżek, L., Wachowski, M., Torzewski, J. The influence of post-weld heat treatment on the microstructure and fatigue properties of Sc-modified AA2519 friction stir-welded joint. Materials 2019; 12(4): 583.
8. Srinivasa, R.M., and Ramanaiah, N. Optimization of Process parameters for FSW of Al-Mg-Mn-Sc-Zr alloy using CCD and RSM. Strojnícky časopis-Journal of Mechanical Engineering 2018; 68(3): 195–224.
9. Jiang, F., Zhou, J., Huang, H., Qu, J. Characterisation of microstructure and mechanical properties in Al-Mg alloy with addition of Sc and Zr. Materials Research Innovations 2014; 18(4): 4–228.
10. Lei, X., Deng, Y., Peng, Y., Yin, Z. Microstructure and properties of TIG/FSW welded joints of a new Al-Zn-Mg-Sc-Zr alloy. Journal of materials engineering and performance 2013; 22: 2723–2729.
11. Peng, Y., Zhimin, Y., Xuefeng, L., Qinglin, P. Microstructure and properties of friction stir welded joints of Al-Mg-Sc alloy plates. Rare Metal Materials and Engineering 2011; 40(2): 201–205.
12. Kumar, K.K., Kumar, A., and Satyanarayana, M.V.N.V. Effect of friction stir welding parameters on the material flow, mechanical properties and corrosion behavior of dissimilar AA5083-AA6061 joints. Proceedings of the Institution of Mechanical Engineers, Part C: Journal of Mechanical Engineering Science 2022; 236(6): 2901–2917.

13. Raturi, M., and Bhattacharya, A. Mechanical strength and corrosion behavior of dissimilar friction stir welded AA7075-AA2014 joints. *Materials Chemistry and Physics* 2021; 262: 124338.
14. Zhang, C., Cao, Y., Huang, G., Zeng, Q. Influence of tool rotational speed on local microstructure, mechanical and corrosion behavior of dissimilar AA2024/7075 joints fabricated by friction stir welding. *Journal of Manufacturing Processes* 2020; 49: 214–226.
15. Sudhakar, U., and J. Srinivas. Mechanical characteristics and corrosion behavior of friction stir AA5251-AA6063 butt welds. *Materials Today: Proceedings* 2019; 15: 132–137.
16. Sinhmar, S., and Dwivedi D.K. A study on corrosion behavior of friction stir welded and tungsten inert gas welded AA2014 aluminium alloy. *Corrosion Science* 2018; 133: 25–35.
17. D'Urso, G., Giardini, C., Lorenzi, S., Cabrini, M., Pastore, T. The effects of process parameters on mechanical properties and corrosion behavior in friction stir welding of aluminum alloys. *Procedia Engineering* 2017; 183: 270–276.
18. Fahimpour, V., Sadrnezhad, S.K., and Karimzadeh, F. Corrosion behavior of aluminum 6061 alloy joined by friction stir welding and gas tungsten arc welding methods. *Materials & Design* 2012; 39: 329–333.
19. Kciuk, M., Kurc, A. and Szewczenko, J. Structure and corrosion resistance of aluminium AlMg2. 5; AlMg5Mn and AlZn5Mg1 alloys. *Journal of Achievements in Materials and Manufacturing Engineering* 2010; 41(1–2): 74–81.
20. Surekha, K., Murty, B.S. and Rao K.P. Effect of processing parameters on the corrosion behaviour of friction stir processed AA 2219 aluminum alloy. *Solid state sciences* 2009; 11(4): 907–917.
21. Jariyaboon, M., Davenport, A.J., Ambat, R., Connolly, B.J., Williams, S.W. Price, D.A. The effect of welding parameters on the corrosion behaviour of friction stir welded AA2024–T351. *Corrosion science* 2007; 49(2): 877–909.
22. Pardo, A., Merino, M.C., Coy, A.E., Arrabal, R. Corrosion behaviour of magnesium/aluminium alloys in 3.5 wt.% NaCl. *Corrosion Science* 2008; 50(3): 823–834.
23. Venugopal, T., Rao, K.S. and Rao, K.P. Studies on friction stir welded AA 7075 aluminum alloy. *Trans. Indian Inst. Met* 2004; 57(6): 659–663.
24. Hannour, F., Davenport, A.J. and Strangwood, M. Corrosion of friction stir welds in high strength aluminium alloys. 2nd International Symposium on Friction Stir Welding 2000.
25. Kasirajan, T., Ravindran, R., Ramkumar, T. and Selvakumar, M. Investigation on microstructural, mechanical and thermal evolution during friction stir welding of dissimilar aluminium alloys. *Transactions of the Canadian Society for Mechanical Engineering* 14 May 2019.
26. Kluz, R., Bucior, M., Kubit, A. Identifying optimal friction stir welding process parameters for 2024 al alloy butt joints. *advances in Science and Technology Research Journal*. December 2019; 13(4): 48–53
27. Zhu, X.-W., Deng, Y., Lai, Y., Guo, Y.-F., Yang, Z.-A., Fu, L., Xu, G.-F., Huang, J.-W. Effects of Al₃(Sc_{1-x}Zr_x) nano-particles on microstructure and mechanical properties of friction-stir-welded Al-Mg-Mn alloys. *Transactions of Nonferrous Metals Society of China* 2023; 33(1): 25–35.
28. Zaki, A., Ul-Hamid, A. and Abdul-Aleem B.J. The corrosion behavior of scandium alloyed Al 5052 in neutral sodium chloride solution. *Corrosion Science* 2001; 43(7): 1227–1243.